Article

One-Bond Spin–Spin Coupling Constants of X–H Proton Donors in Complexes with X–H–Y Hydrogen Bonds, for X = C, N, O, and F: Predictions, Comparisons, and Relationships among *J*, *K*, and X–H Distances

Janet E. Del Bene, and Jos Elguero

J. Am. Chem. Soc., **2004**, 126 (47), 15624-15631• DOI: 10.1021/ja0401545 • Publication Date (Web): 09 November 2004

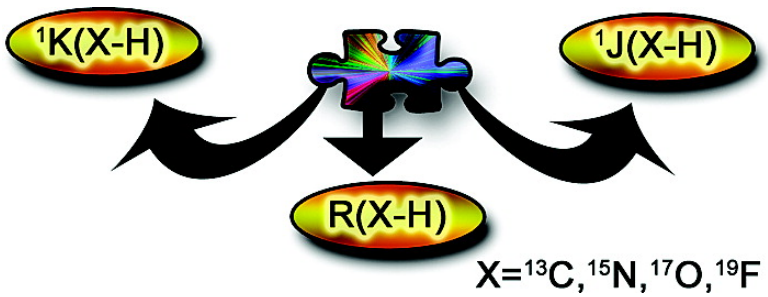

More About This Article

Additional resources and features associated with this article are available within the HTML version:

- Supporting Information
- Links to the 6 articles that cite this article, as of the time of this article download
- Access to high resolution figures
- Links to articles and content related to this article
- Copyright permission to reproduce figures and/or text from this article

View the Full Text HTML

J|A|C|S
ARTICLES
Published on Web 11/09/2004

One-Bond Spin−Spin Coupling Constants of X−^{1}H Proton Donors in Complexes with X−H−Y Hydrogen Bonds, for X = ^{13}C, ^{15}N, ^{17}O, and ^{19}F: Predictions, Comparisons, and Relationships among $^1J_{X-H}$, $^1K_{X-H}$, and X−H Distances

Janet E. Del Bene*,† and José Elguero‡

Contribution from the Department of Chemistry, Youngstown State University, Youngstown, Ohio 44555 and Instituto de Química Médica, CSIC, Juan de la Cierva, 3, E-28006 Madrid, Spain

Received June 16, 2004; E-mail: jedelbene@ysu.edu

Abstract: Ab initio calculations at the equation-of-motion coupled cluster (EOM-CCSD) level of theory have been carried out to investigate one-bond ^{13}C−^{1}H, ^{15}N−^{1}H, ^{17}O−^{1}H, and ^{19}F−^{1}H coupling constants in a systematic study of monomers and hydrogen-bonded complexes. Computed coupling constants ($^1J_{X-H}$) for monomers are in good agreement with available experimental data. All reduced Fermi-contact terms and reduced coupling constants ($^1K_{X-H}$) for monomers and complexes are positive. Plots of $^1K_{X-H}$ versus the X−H distance for the 16 monomers and the 64 complexes in which these monomers are proton donors exhibit significant scatter. However, a linear relationship has been demonstrated for the first time between coupling constants and X−H distances for different X atoms by plotting the ratios of the coupling constants for complexes and corresponding monomers versus the ratios of distances for complexes and corresponding monomers times the square of the Pauling electronegativity. Since the ratio removes the dependence of coupling constants on the magnetogyric ratios of X, this relationship holds for both $^1K_{X-H}$ and $^1J_{X-H}$. The decrease in reduced coupling constants ($^1K_{X-H}$) as the X−H distance increases is due primarily to the increased proton-shared character of the hydrogen bond.

Introduction

In a recent paper, we reported a systematic investigation of the signs of two-bond reduced X−Y Fermi-contact terms and total spin−spin coupling constants ($^{2h}K_{X-Y}$) for complexes with X−H−Y hydrogen bonds, for X and/or Y the second-period elements ^{13}C, ^{15}N, ^{17}O, and ^{19}F.[1] These complexes are stabilized by C−H−N, N−H−N, O−H−N, F−H−N, C−H−O, O−H−O, O−H−F, and C−H−F hydrogen bonds. (Complexes with F−H−F hydrogen bonds are not included in this list, but these have been discussed in previous studies).[2,3] Except for the reduced F−F coupling constant in $(HF)_2$, all reduced two-bond spin−spin coupling constants $^{2h}K_{X-Y}$ are positive. Thus, it is possible to predict the sign of $^{2h}J_{X-Y}$ for a given complex by simply noting the signs of the magnetogyric ratios of X and Y. If neither or both X and Y have negative magnetogyric ratios, $^{2h}J_{X-Y}$ is positive; if either X or Y has a negative magnetogyric ratio, $^{2h}J_{X-Y}$ is negative. Since the signs and magnitudes of $^{2h}J_{X-Y}$ for these complexes are determined by the Fermi-contact term which is an order of magnitude greater than any other term,[4−8] insights into the positive signs of the reduced Fermi-contact terms and $^{2h}K_{X-Y}$ were obtained from the Nuclear Magnetic Resonance Triplet Wave function Model (NMRTWM).[9] The study of two-bond coupling constants in complexes has led us to investigate the corresponding one-bond X-^{1}H coupling constants with X = ^{13}C, ^{15}N, ^{17}O, and ^{19}F for a group of isolated monomers and hydrogen-bonded complexes in which these monomers are the proton donors. The results of that investigation are the subject of this paper.

Methods

Structures of both the proton-donor monomers and the hydrogen-bonded complexes were obtained in previous studies at second-order Møller−Plesset perturbation theory[10−13] with the 6-31+G(d,p) basis set[14−17] [MP2/6-31+G(d,p)]. Coupling constants were computed using the equation-of-motion coupled cluster singles and doubles method (EOM-CCSD) in the CI−

† Department of Chemistry, Youngstown State University.
‡ Instituto de Química Médica, CSIC.

(1) Del Bene, J. E.; Elguero, J. *Magn. Reson. Chem.* **2004**, *42*, 421.
(2) Del Bene, J. E.; Jordan, M. J. T.; Perera, S. A.; Bartlett, R. J. *J. Phys. Chem. A.* **2001**, *105*, 8399.
(3) Del Bene, J. E.; Elguero, J.; Alkorta, I.; Yáñez, M.; Mó, O. J. *Chem. Phys.* **2004**, *120*, 3237.
(4) Del Bene, J. E.; Perera, S. A.; Bartlett, R. J. *J. Chem. Phys. A.* **2001**, *105*, 930.
(5) Del Bene, J. E.; Perera, S. A.; Bartlett, R. J. *Magn. Reson. Chem.* **2001**, *39*, S109.
(6) Del Bene, J. E.; Perera, S. A.; Bartlett, R. J.; Yáñez, M.; Mó, O.; Elguero, J.; Alkorta, I. *J. Phys. Chem. A.* **2003**, *107*, 3121.
(7) Del Bene, J. E.; Perera, S. A.; Bartlett, R. J.; Mó, O.; Yáñez, M; Elguero, J.; Alkorta, I. *J. Phys. Chem. A.* **2003**, *107*, 3126.
(8) Del Bene, J. E.; Perera, S. A.; Bartlett, R. J.; Mó, O.; Yáñez, M.; Elguero, J.; Alkorta, I. *J. Phys. Chem. A.* **2003**, *107*, 3222.
(9) Del Bene, J. E.; Elguero, J. *Chem. Phys. Lett.* **2003**, *382*, 100.
(10) Pople, J. A.; Binkley, J. S.; Seeger, R. *Int. J. Quantum Chem. Quantum Chem.Symp.* **1976**, *10*, 1.
(11) Krishnan, R.; Pople, J. A. *Int. J. Quantum Chem.* **1978**, *14*, 91.
(12) Bartlett, R. J.; Silver, D. M. *J. Chem. Phys.* **1975**, *62*, 3258.
(13) Bartlett, R. J.; Purvis, G. D. *Int. J. Quantum Chem.* **1978**, *14*, 561.

10.1021/ja0401545 CCC: $27.50

(configuration interaction) like approximation,[18−21] correlating all electrons. For these calculations, the Ahlrichs[22] qzp basis set was placed on C, N, O, and F atoms, qz2p on the hydrogen-bonded hydrogen, and the Dunning cc-pVDZ basis[23,24] on other hydrogens. If in a monomer there are two or more equivalent hydrogen atoms which could be hydrogen-bonded, they were treated equivalently by placing the same qz2p basis set on each. No assumptions have been made concerning the relative importance of the various terms which contribute to the total coupling constants for monomers and complexes. Rather, the paramagnetic spin−orbit (PSO), diamagnetic spin−orbit (DSO), Fermi-contact (FC), and spin-dipole (SD) terms have been computed for all but one monomer and for the majority of hydrogen-bonded complexes.

The absolute shieldings (σ, ppm) of hydrogen-bonded protons were calculated for NH_4^+ and complexes in which NH_4^+ is the proton donor using the GIAO (gauge-invariant atomic orbitals) formalism,[25] at the MP2 level with the same basis sets used for the coupling constant calculations. Structure determinations were done using the Gaussian 98 suite of programs,[26] and coupling constants were computed using ACES II.[27] All calculations were performed on the Cray SV1 or the Itanium cluster at the Ohio Supercomputer Center.

Results and Discussion

Monomers. The proton donors are grouped in Table 1 under C−H, N−H, O−H, and F−H donors. Included among these are examples of neutral and cationic donors, and donors with different hybridizations of C, N, O, and F. The N−H donors comprise the most extensive set, including neutral molecules that have nitrogen atoms that are sp (HNC), sp^2 (pyrrole), or sp^3 (NH_3) hybridized; and cations that have sp ($HCNH^+$), sp^2 (pyridinium), or sp^3 (NH_4^+) hybridized nitrogens. Table 1 reports the monomer X−H distances, the computed values of the PSO, DSO, FC, and SD terms, and computed and experimental[28−35] $^1J_{X-H}$ values. It is apparent from the computed results that the Fermi-contact term is the dominant term contributing to $^1J_{X-H}$. Moreover, for all C−H, N−H, and O−H donors except H_2O, the FC term is more than an order of magnitude greater than any other term. However, it does appear that the dominance of the FC term decreases in the monomers as the number of lone pairs of electrons on X increases. (Pecul, Sadlej, and Helgaker have noted in a methodological study that the performance of DFT deteriorates as the number of electron pairs on the coupled atoms increases).[36] Thus, the FC term for C−H coupling approximates $^1J_{C-H}$ to better than 1%; the FC term approximates $^1J_{N-H}$ and $^1J_{O-H}$ to within 5% except for H_2O, in which case FC underestimates (in an absolute sense) $^1J_{O-H}$ by 15% due to the contribution of the PSO term. The FC term is a poor approximation to $^1J_{F-H}$ in both FH and FH_2^+ due to the large positive values of the PSO term.

Table 1. Computed X−H Distances (Å) and Coupling Constants ($^1J_{X-H}$) and Its Components (Hz), and Experimental $^1J_{X-H}$ Values for Monomers Which May Be Proton Donors in Hydrogen-Bonded Complexes

	R(X–H)	PSO	DSO	FC	SD	$^1J_{X-H}$	$^1J_{X-H}$ (exptl)
				C−H			
HCN	1.067	−0.5	0.4	251.4	0.4	251.7	269[a]
CH_2F_2	1.086	−0.6	1.1	171.3	0.2	172.0	167.5[b]
$HCNH^+$	1.079	−1.2	0.3	332.5	0.9	332.5	320[a]
OCH^+	1.091	−0.9	0.4	345.0	1.1	345.6	[c]
				N−H			
HNC	1.000	−0.8	−0.2	−114.4	−0.4	−115.8	
pyrrole	1.007	−1.9	−0.4	−90.8	−0.3	−93.4	−96.5[d]
NH_3	1.011	−2.8	−0.1	−58.4	−0.3	−61.6	−61.2[e]
$HCNH^+$	1.017	0.4	−0.2	−149.0	−0.5	−149.3	−134[f]
pyridinium	1.017			−91.6		−91.6[g]	−90.5[f]
NH_4^+	1.022	−1.5	−0.1	−73.4	0.0	−75.0	−73.3[e]
				O−H			
H_2O	0.963	−11.2	−0.1	−65.9	−0.7	−77.9	−96[h]
COH^+	0.997	−2.2	−0.3	−180.6	−0.6	−183.7	
H_2COH^+	0.985	−3.8	−0.2	−86.2	−0.1	−90.3	
H_3O^+	0.980	−5.6	−0.1	−115.1	0.1	−120.7	
				F−H			
HF	0.926	184.0	0.4	309.3	1.7	495.4	529[i]
FH_2^+	0.969	81.6	−0.2	556.6	−6.6	631.4	

[a] Ref 28. [b] Ref 29. [c] Reported as not measurable in ref 30. [d] Ref 31. [e] Ref 32. [f] Ref 33. [g] Estimated from the Fermi-contact term. [h] Ref 34. [i] Ref 35.

From Table 1 it can be seen that for the neutral N−H donor molecules, the N−H bond length increases and $^1J_{N-H}$ decreases (in an absolute sense) as the hybridization changes from sp to sp^2 to sp^3; however this simple relationship does not hold in general. For the cationic N−H donors, the sp-hybridized donor $HCNH^+$ has the same N−H distance as the sp^2 donor pyridinium, but the computed N−H coupling constants are very different at −149.3 and −91.6 Hz, respectively. These computed values are in agreement with the experimental values of −134

(14) Hehre, W. J.; Ditchfield, R.; Pople, J. A. *J. Chem. Phys.* **1982**, *56*, 2257.
(15) Hariharan, P. C.; Pople, J. A. *Theor. Chim. Acta* **1973**, *238*, 213.
(16) Spitznagel, G. W.; Clark, T.; Chandrasekhar, J.; Schleyer, P. v. R. *J. Comput. Chem.* **1982**, *3*, 3633.
(17) Clark, T.; Chandrasekhar, J.; Spitznagel, G. W.; Schleyer, P. v. R. *J. Comput. Chem.* **1983**, *4*, 294.
(18) Perera, S. A.; Sekino, H.; Bartlett, R. J. *J. Chem. Phys.* **1994**, *101*, 2186.
(19) Perera, S. A.; Nooijen, M.; Bartlett, R. J. *J. Chem. Phys.* **1996**, *104*, 3290.
(20) Perera, S. A.; Bartlett, R. J. *J. Am. Chem. Soc.* **1995**, *117*, 8476.
(21) Perera, S. A.; Bartlett, R. J. *J. Am. Chem. Soc.* **1996**, *118*, 7849.
(22) Schäfer, A.; Horn, H.; Ahlrichs, R. *J. Chem. Phys.* **1992**, *97*, 2571.
(23) Dunning, T. H., Jr. *J. Chem. Phys.* **1989**, *90*, 1007.
(24) Woon, D. E.; Dunning, T. H., Jr. *J. Chem. Phys.* **1995**, *103*, 4572.
(25) Ditchfield, R. *Mol. Phys.* **1974**, *27*, 789. London, F. J. *Phys. Radium.* **1937**, *8*, 397.
(26) Frisch, M. J.; Trucks, G. W.; Schlegel, H. B.; Scuseria, G. E.; Robb, M. A.; Cheeseman, J. R.; Zakrzewski, V. G.; Montgomery, J. A., Jr.; Stratmann, R. E.; Burant, J. C.; Dapprich, S.; Millam, J. M.; Daniels, A. D.; Kudin, K. N.; Strain, M. C.; Farkas, O.; Tomasi, J.; Barone, V.; Cossi, M.; Cammi, R.; Mennucci, B.; Pomelli, C.; Adamo, C.; Clifford, S.; Ochterski, J.; Petersson, G. A.; Ayala, P. Y.; Cui, Q.; Morokuma, K.; Malick, D. K.; Rabuck, A. D.; Raghavachari, K.; Foresman, J. B.; Cioslowski, J.; Ortiz, J. V.; Baboul, A. G.; Stefanov, B. B.; Liu, G.; Liashenko, A.; Piskorz, P.; Komaromi, I.; Gomperts, R.; Martin, R. L.; Fox, D. J.; Keith, T.; Al-Laham, M. A.; Peng, C. Y.; Nanayakkara, A.; Gonzalez, M.; Challacombe, M.; Gill, P. M. W.; Johnson, B.; Chen, W.; Wong, M. W.; Andres, J. L.; Gonzalez, C.; Head-Gordon, M.; Replogle, E. S.; Pople, J. A. Gaussian 98, Rev. A9, Gaussian, Inc. Pittsburgh, Pa, 1998.
(27) ACES II is a program product of the Quantum Theory Project, University of Florida. Authors: Stanton, J. F.; Gauss, J.; Watts, J. D.; Nooijen, M.; Oliphant, N.; Perera, S. A.; Szalay, P. G.; Lauderdale, W. J.; Gwaltney, S. R.; Beck, S.; Balkova, A.; Bernholdt, D. E.; Baeck, K.−K.; Tozyczko, P.; Sekino, H.; Huber, C.; Bartlett, R. J. Integral packages included are VMOL (Almlof, J.; Taylor, P. R.); VPROPS (Taylor, P. R.); ABACUS (Helgaker, T.; Jensen, H. J. Aa.; Jorgensen, P.; Olsen, J.; Taylor, P. R.). Brillouin-Wigner perturbation theory was implement by Pittner, J.
(28) Stothers, J. B. Carbon-13 NMR Spectroscopy, Academic Press: New York, 1972, p. 345.
(29) Waser, R.; Diehl, P. *Magn. Reson. Chem.* **1987**, *25*, 766.
(30) Sørensen, T. S. *Angew. Chem., Int. Ed. Engl.* **1998**, *37*, 603.
(31) Berger, S.; Braun, S.; Kalinowski, H.-O. *NMR Spectroscopy of the Non-Metallic Elements*; John Wiley & Sons: Chichester, 1997, p 246.
(32) Berger, S.; Braun, S.; Kalinowski, H.-O. *NMR Spectroscopy of the Non-Metallic Elements*; John Wiley & Sons: Chichester, 1997, p 245.
(33) Berger, S.; Braun, S.; Kalinowski, H.-O. *NMR Spectroscopy of the Non-Metallic Elements*; John Wiley & Sons: Chichester, 1997, p 247.
(34) Berger, S.; Braun, S.; Kalinowski, H.-O. NMR Spectroscopy of the Non-Metallic Elements, John Wiley & Sons: Chichester, 1997, p 386.
(35) Berger, S.; Braun, S.; Kalinowski, H.-O. NMR Spectroscopy of the Non-Metallic Elements, John Wiley & Sons: Chichester, 1997, p 587.
(36) Pecul, M.; Sadlej, J.; Helgaker, T. *Chem. Phys. Lett.* **2003**, *372*, 476.

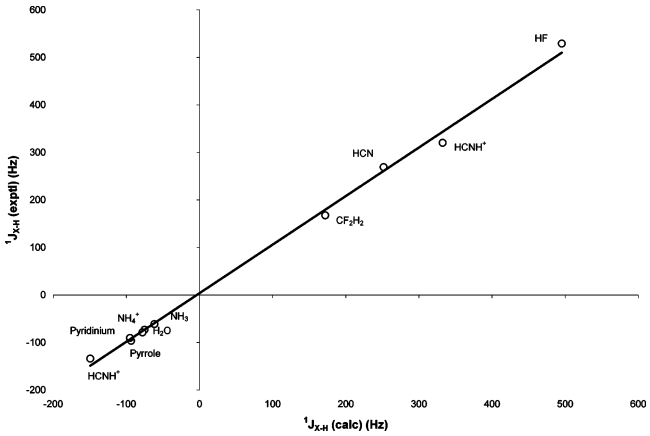

Figure 1. Experimental versus computed values of the one-bond X−H spin−spin coupling constants ($^1J_{X-H}$).

and −90.5 Hz, respectively, reported by Berger et al.[33] Cationic N−H coupling constants decrease (in an absolute sense) in the order $HCNH^+$ (sp) > pyridinium (sp^2) > NH_4^+ (sp^3). For the cations with O−H bonds the order of decreasing O−H distance is COH^+ (sp) > H_2COH^+ (sp^2) > H_3O^+ (sp^3), but the order of decreasing (in an absolute sense) $^1J_{O-H}$ is COH^+ (sp) > H_3O^+ (sp^3) > H_2COH^+ (sp^2).

The experimental values of $^1J_{X-H}$ for ten X−H donor molecules are plotted against the computed values in Figure 1. The coupling constants vary over a wide range, from −200 Hz to + 500 Hz. The equation of the straight line shown in Figure 1 is

$$^1J_{X-H}\,(\text{exptl}) = (1.02 \pm 0.02)\,^1J_{X-H}\,(\text{calcd}) \qquad (1)$$

with a correlation coefficient of 0.997. The largest differences between computed and experimental values are found for $HCNH^+$ (11%) and for HCN and HF (6%). The overall agreement between theory and experiment is really quite good. (It should be noted that the calculations were carried out at equilibrium geometries, whereas the experimental data refer to vibrational ground-state geometries. However, changes in X−H distances due primarily to zero-point motion associated with the anharmonic X−H stretching mode have a relatively small effect on X−H coupling constants.[37,38]). Both ab initio and DFT studies of coupling constants involving small molecules have been reported recently.[37−42] These include a very recent investigation by Wu, Gräfenstein, and Cremer[42] of reduced X−H coupling constants for a series of second- and third-row hydrides including NH_3, H_2O, and HF. Their results were obtained using their CPDFT procedure with the B3LYP and BLYP functionals and the 6-311G(d,p) basis set. Their computed values for X−H coupling constants for these three molecules are 41.5 (46.3 with Dunning's cc-pV5Z basis), 34.3, and 26.3 ($\times 10^{19}$ N A^{-2} m^{-3}), respectively. Our EOM-CCSD values in the same units are 50.6, 47.8, and 43.8, in better agreement with the experimental values of 50.3,[31] 58.9,[33] and 46.8,[34] respectively. The difficulty in describing coupling constants for atoms with lone pairs of electrons noted in ref 36 is again manifest in the results reported in ref 42.

It is significant that $^1J_{X-H}$ for $^{15}N-^1H$ and $^{17}O-^1H$ appear in the lower-left quadrant of Figure 1, indicating that the computed and experimental signs of these coupling constants are negative. $^1J_{X-H}$ for $^{13}C-^1H$ and $^{19}F-^1H$ appear in the upper right, corresponding to positive values of both computed and experimental coupling constants. Analysis of the signs of these coupling constants will be presented below.

Complexes. Table 2 presents computed X−H distances, FC terms, and $^1J_{X-H}$ for the monomers and complexes investigated in this study. The complexes are grouped according to the nature of the X−H donor, in the order C−H, N−H, O−H, F−H. Within these four groups, neutral complexes are listed first according to the hybridization of X (sp, sp^2, sp^3), and these are followed by cationic complexes again listed according to the hybridization of X. Under a particular proton-donor molecule or ion, the complexes are listed in order of increasing X−H distance. A cursory examination of Table 2 shows that the FC term is an excellent approximation to $^1J_{X-H}$ for complexes in which X−H is either C−H or N−H. This approximation is not as good for complexes with O−H as the donor, especially when the donor molecule is H_2O. The FC term is a poor approximation to $^1J_{F-H}$, especially for complexes in which the neutral HF molecule is the proton donor.

To compare X−H coupling constants in complexes with different proton donors, coupling constants $^1J_{X-H}$ have been converted to reduced coupling constants $^1K_{X-H}$,[43] and these are also reported in Table 2. The scattergram (Figure 2) shows $^1K_{X-H}$ values versus X−H distances. There are two very striking observations that can be made from this figure. The first is that there appears to be little if any correlation between X−H distances and reduced X−H coupling constants. The second is that all one-bond reduced X−H coupling constants ($^1K_{X-H}$) are positive.

Figure 2 illustrates that there is significant scatter in the values of reduced X−H coupling constants as a function of the X−H distances. Table 2 also illustrates this point. For example, in the complexes with NH_4^+ as the proton donor, the Fermi-contact term and $^1J_{N-H}$ increase in absolute value in the order NH_4^+ < NH_4^+:OC ≅ NH_4^+:FH, even though the N−H distances increase in this order. Moreover, the complex NH_4^+:CO in which the N−H distance is 1.035 Å has a coupling constant that is similar to NH_4^+, which has an N−H distance of 1.022 Å.

To gain insight into the variation of $^1J_{X-H}$ with X−H distance, we have examined $^1J_{N-H}$ in the NH_4^+ cation and its complexes as a function of the N−H distance. For the cation NH_4^+, $^1J_{N-H}$ was computed for the stretched N−H bond. The distances selected correspond to the N−H distances in the hydrogen-bonded complexes listed in Table 2 that have NH_4^+ as the proton donor. Figure 3 presents two graphs: one for $^1J_{N-H}$ for the stretched N−H bond in NH_4^+, and the other for $^1J_{N-H}$ for the complexes with NH_4^+ as the proton donor. It is apparent that $^1J_{N-H}$ in the isolated cation is nearly constant over the relatively short range of N−H distances considered, decreasing only slightly in absolute value as the N−H distance increases from 1.022 to 1.113 Å. The near constancy of $^1J_{N-H}$ reflects the

(37) Ruden, T. A.; Lutnæs, O. B.; Helgaker, T.; Ruud, K. *J. Chem. Phys.* **2003**, *118*, 9572.
(38) Wigglesworth, R. D.; Raynes, W. T.; Sauer, S. P. A.; Oddershede, *J. Mol. Phys.* **1998**, *94*, 851.
(39) Enevoldsen, T.; Oddershede, J.; Sauer, S. P. A. *Theor. Chem. Acta* **1998**, *100*, 275.
(40) Auer, A. A.; Gauss, J. *J. Chem. Phys.* **2001**, *115*, 1619.
(41) Peralta, J. E.; Scuseria, G. E.; Cheeseman, J. R.; Frisch, M. J. *Chem. Phys. Lett.* **2003**, *375*, 452.
(42) Wu, A.; Gräfenstein, J.; Cremer, D. *J. Phys. Chem. A* **2003**, *107*, 7043.
(43) Raynes, W. T. *Magn. Reson. Chem.* **1992**, *30*, 686.

Table 2. Computed X−H Distances (Å), X−^{1}H Fermi Contact Terms (FC) and Total Coupling Constants [$^1J_{X-H}$ (Hz)], and Reduced Coupling Constants [$^1K_{X-H}$ (N A^{-2} m^{-3})] for X−H−Y Hydrogen Bonds, with X = ^{13}C, ^{15}N, ^{17}O, and ^{19}F

complexes with C–H donors		R(C–H)	FC	$^1J_{C-H}$	$^1K_{C-H}$ (×10^{19})	complexes with C–H donors		R(C–H)	FC	$^1J_{C-H}$	$^1K_{C-H}$ (×10^{19})
1	*NCH*	1.067	251.4	251.7	83.3	13	*HNCH*$^+$	1.079	332.5	332.5	110.1
2	NCH:OC	1.067	252.2	252.5	83.6	14	HNCH$^+$:OC	1.086	327.4	327.7	108.5
3	NCH:FH	1.069	253.8	254.1	84.1	15	HNCH$^+$:FH	1.091	324.8	325.3	107.7
4	NCH:NCH	1.072	254.4	254.7	84.3	16	HNCH$^+$:CO	1.100	321.0	321.6	106.5
5	NCH:NH$_3$	1.081	252.7	253.0	83.7	17	HNCH$^+$:NCH	1.129	299.2	300.1	99.3
6	NCH:pyridine	1.082	251.9	251.9[a]	83.4	18	HNCH$^+$:CNH ($C_{\infty v}$)	1.146	288.6	289.9	96.0
7	NCH:NC$^-$	1.110	248.6	249.3	82.5	19	HNCH$^+$:CNH ($D_{\infty h}$)	1.376	130.8	132.7	43.9
8	NCH:CN$^-$ ($C_{\infty v}$)	1.114	248.0	248.7	82.3	20	*OCH*$^+$	1.091	345.0	345.6	114.4
9	NCH:CN$^-$ ($D_{\infty h}$)	1.391	99.9	101.3	33.5	21	OCH$^+$:OC	1.109	330.3	331.4	109.7
10	*CF$_2$H$_2$*	1.086	171.3	172.0	56.9	22	OCH$^+$:CO ($C_{\infty v}$)	1.160	292.6	294.3	97.4
11	F$_2$HCH:OCH$_2$	1.083	178.5	178.5[a]	59.1	23	OCH$^+$:FH	1.121	319.5	320.7	106.2
12	F$_2$HCH:OH$_2$	1.084	180.8	181.5	60.1						

complexes with N–H donors		*R*(N–H)	FC	$^1J_{N-H}$	$^1K_{N-H}$ (×10^{19})	complexes with N–H donors		*R*(N–H)	FC	$^1J_{N-H}$	$^1K_{N-H}$ (×10^{19})
24	*CNH*	1.000	−114.4	−115.8	95.1	38	HCNH$^+$:FH	1.046	−136.7	−136.9	112.4
25	CNH:NCH	1.012	−114.9	−115.7	95.0	39	(HCN)$_2$H$^+$ ($D_{\infty h}$)	1.261	−56.6	−56.9	46.7
26	CNH:NH$_3$	1.035	−109.2	−109.2[a]	89.7	40	*Pyridinium*	1.017	−91.6	−91.6[a]	75.2
27	CNH:pyridine	1.040	−107.4	−107.4[a]	88.2	41	Pyridinium:FH	1.021	−93.2	−93.2[a]	76.5
28	CNH:NC$^-$ ($C_{\infty v}$)	1.141	−79.2	−79.5	65.3	42	Pyridinium:NCH	1.035	−92.0	−92.0[a]	75.6
29	CNH:NC$^-$ ($D_{\infty h}$)	1.268	−43.1	−43.4	35.6	43	Pyridium:CNH	1.042	−90.7	−90.7[a]	74.5
30	*Pyrrole*	1.007	−90.8	−93.4	76.7	44	*NH$_4$*$^+$	1.022	−73.4	−75.0	61.6
31	Pyrrole:NCH	1.011	−93.6	−93.6	76.9	45	NH$_4$$^+$:OC	1.027	−74.4	−75.8	62.3
32	Pyrrole:NH$_3$	1.021	−93.7	−93.7[a]	77.0	46	NH$_4$$^+$:FH	1.029	−74.5	−75.9	62.3
33	*NH$_3$*	1.011	−58.4	−61.6	50.6	47	NH$_4$$^+$:CO	1.035	−73.7	−75.0	61.6
34	NH$_3$:NH$_2$$^-$ (C_1)	1.052	−63.2	−64.4	52.9	48	NH$_4$$^+$:NCH	1.049	−72.7	−73.7	60.5
35	NH$_3$:NH$_2$$^-$ (C_2)	1.304	−22.0	−22.0	18.1	49	NH$_4$$^+$:CNH	1.057	−71.2	−72.1	59.2
36	*HCNH*$^+$	1.017	−149.0	−149.3	122.6	50	NH$_4$$^+$:NH$_3$ (C_{3v})	1.113	−60.5	−61.2	50.3
37	HCNH$^+$:OC	1.033	−142.0	−142.2	116.8	51	NH$_4$$^+$:NH$_3$ (D_{3d})	1.299	−26.4	−26.5	21.8

complexes with O–H donors		*R*(O–H)	FC	$^1J_{O-H}$	$^1K_{O-H}$ (×10^{19})	complexes with O–H donors		*R*(O–H)	FC	$^1J_{O-H}$	$^1K_{O-H}$ (×10^{19})
52	*H$_2$O*	0.963	−65.9	−77.9	47.8	60	*H$_2$COH*$^+$	0.985	−86.2	−90.3	55.4
53	HOH:NCH	0.967	−70.2	−80.3	49.3	61	H$_2$CO$_2$H$^+$:FH	1.006	−85.1	−87.7	53.8
54	HOH:OH$_2$	0.970	−71.6	−81.0	49.7	62	(H$_2$CO)$_2$H$^+$ (C_{2h})	1.205	−27.7	−27.8	17.1
55	HOH:NC$^-$	0.992	−74.2	−80.5	49.4	63	*H$_3$O*$^+$	0.980	−115.1	−120.7	74.1
56	HOH:OH$^-$ (C_1)	1.096	−49.5	−51.6	31.7	64	H$_2$OH$^+$:FH	1.011	−106.8	−110.1	67.6
57	HOH:OH$^-$ (C_2)	1.222	−19.9	−20.1	12.3	65	H$_2$OH$^+$:CO	1.039	−97.2	−99.6	61.1
58	*COH*$^+$	0.997	−180.6	−183.7	112.8	66	H$_2$OH$^+$:NCH	1.134	−64.7	−65.1	40.0
59	(CO)$_2$H$^+$ ($D_{\infty h}$)	1.197	−68.0	−68.2	41.9	67	H$_2$OH$^+$OH$_2$ (C_2)	1.194	−47.5	−47.5	29.2

complexes with F–H donors		*R*(F–H)	FC	$^1J_{F-H}$	$^1K_{F-H}$ (×10^{19})	complexes with F–H donors		*R*(F–H)	FC	$^1J_{F-H}$	$^1K_{F-H}$ (×10^{19})
68	*FH*	0.926	309.3	495.4	43.8	75	FH:NCLi	0.955	356.4	470.1	41.6
69	FH:CO	0.922	353.4	518.6	45.9	76	FH:NH$_3$	0.963	325.5	431.5	38.2
70	FH:NCH	0.927	370.2	516.7	45.7	77	FHF$^-$	1.150	82.1	101.2	9.0
71	FH:OC	0.928	323.9	497.6	44.0	78	*FH$_2$*$^+$	0.969	556.6	631.4	55.8
72	FH:FH	0.932	338.1	497.8	44.0	79	HFH$^+$:OC	1.093	299.4	315.8	27.9
73	FH:OCH$_2$	0.943	341.0	476.8	42.2	80	HFH$^+$:FH (C_{2h})	1.151	186.3	195.3	17.3
74	FH:OH$_2$	0.943	349.0	482.8	42.7						

[a] Estimated from the Fermi-contact term.

absence of an explicit distance-dependent term in the Fermi-contact operator.[44] However, $^1J_{N-H}$ eventually goes to zero as the N−H distance increases, due to a cancellation of positive and negative contributions to the Fermi-contact term from the manifold of excited triplet states that couple to the ground state.[9] In contrast, $^1J_{N-H}$ for the complexes decreases dramatically as the N−H distance increases from 1.027 Å in NH$_4$$^+$:OC to 1.113 Å in N$_2H_7$$^+$, as evident from Figure 3. This suggests that in hydrogen-bonded complexes it is not only the N−H distance which is a factor in determining $^1J_{N-H}$, but also the nature of the hydrogen bond. It is well-known that formation of an X−H−Y hydrogen bond is associated with charge transfer from the proton acceptor to the proton donor moiety. In the process, the ground-state electron densities of X and Y increase, while that of the hydrogen-bonded proton decreases. Since in the sum-over-states expression for the Fermi-contact term (and thus $^1J_{N-H}$), contributions arise from σ-type excited triplet states that couple to the ground state,[44] it can be inferred that the lower

(44) Kirpekar, S.; Jensen, H. J. Aa.; Oddershede, J. *Chem. Phys.* **1994**, *188*, 171.

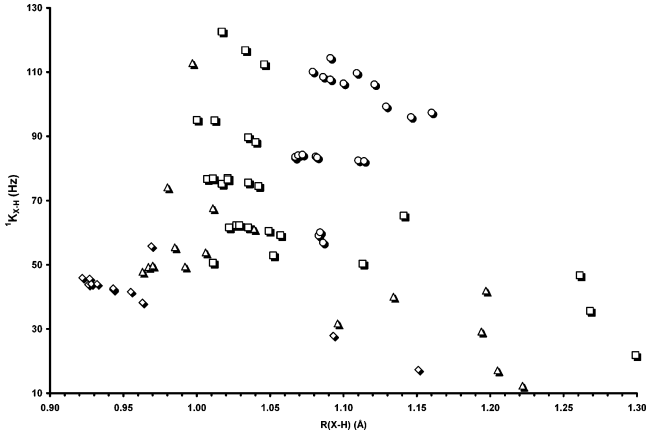

Figure 2. Scattergram showing the values of $^1K_{X-H}$ versus the X−H distance for all monomers and complexes listed in Table 2. ○: C−H □: N−H △: O−H ◇: F−H.

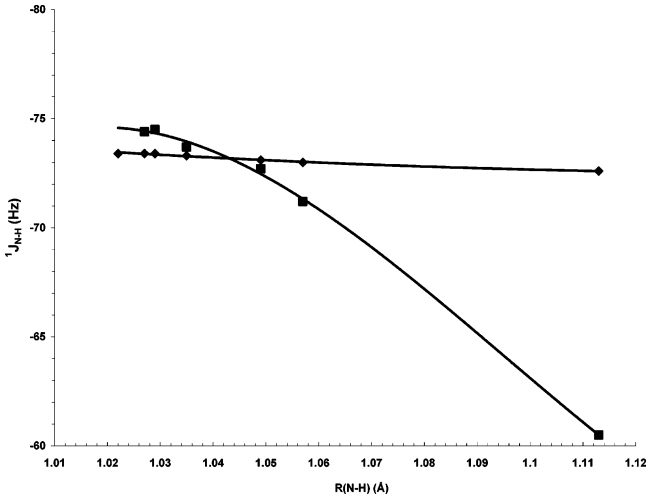

Figure 3. One-bond N−H coupling constants ($^1J_{N-H}$) versus the N−H distance for the stretched N−H bond in NH_4^+ and for the hydrogen-bonded N−H bond in complexes with NH_4^+ as the proton donor ◆ NH_4^+ ■ Hydrogen-bonded complexes with NH_4^+ as the proton donor.

ground-state electron density at the hydrogen-bonded proton is responsible at least in part for the decrease in $^1J_{N-H}$ as the N−H distance increases. As this distance increases, the degree of proton-shared character of the hydrogen bond increases.

In support of this explanation, the shielding constants of the H atom of the stretched N−H bond in the cation NH_4^+ and of the hydrogen-bonded proton in the complexes with NH_4^+ as the donor have been computed, and these are plotted as a function of the N−H distance in Figure 4. A behavior similar to that shown for $^1J_{N-H}$ in Figure 3 is observed. As the N−H distance increases from 1.027 to 1.113 Å in the isolated NH_4^+ cation, the shielding of the H atom of the stretched N−H bond changes slightly from 26.8 to 23.7 ppm. In contrast, as the N−H distance increases in the complexes the shielding decreases from 25.9 ppm in NH_4^+:OC to 13.4 ppm in $N_2H_7^+$. The hydrogen bond in the equilibrium C_{3v} structure of $N_2H_7^+$ has significant proton-shared character, and the hydrogen-bonded H atom has a relatively low electron density.

To further illustrate the point that $^1J_{N-H}$ does not explicitly depend on the N−H distance but is also influenced by the nature of the hydrogen bond, two graphs that show the dependence of $^1J_{N-H}$ on N−N and N−H distances in the complex CNH:NCH are presented in Figure 5.

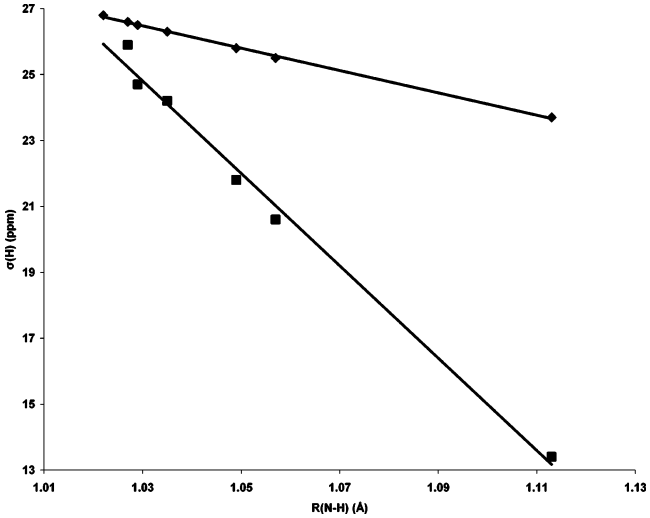

Figure 4. Proton shieldings constants for the stretched N−H bond in NH_4^+ and for the hydrogen- bonded hydrogen in complexes with NH_4^+ as the proton donor ◆ NH_4^+ ■ Hydrogen-bonded complexes with NH_4^+ as the proton donor.

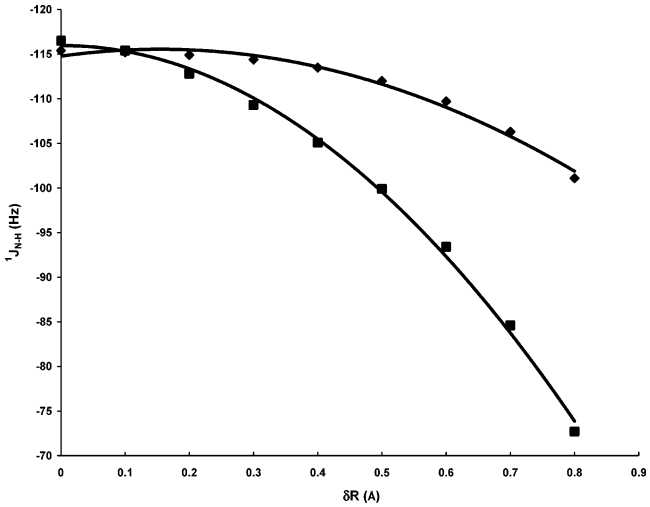

Figure 5. One-bond N−H coupling constants versus N−H and N−N distances in CNH:NCH ◆ N−H distance fixed at 1.012 Å. $\delta R = 0$ Å corresponds to an N−N distance of 3.20 Å, which decreases by 0.1 Å as δR increases to 0.80 Å. At $\delta R = 0.80$, the N−N distance is 2.40 Å. ■ N−N distance fixed at 3.30 Å. The N−H distance increases from 0.90 Å at $\delta R = 0$ Å to 1.70 Å at $\delta R = 0.80$ Å.

In this figure, the proton-shared character of the hydrogen bond increases as δR increases. The top curve is the curve generated by fixing the N−H distance at 1.012 Å, and varying the N−N distance from 2.40 to 3.20 Å in steps of 0.10 Å. In Figure 5, the point for CNH:NCH that corresponds to an N−N distance of 3.20 Å is found at δR = 0.00 Å. This distance then decreases in steps of 0.10 Å until the N−N distance is 2.40 Å when δR = 0.80 Å. Thus, as δR increases, the N−N distance decreases, the difference between the two N−H distances decreases, and the proton-shared character of the hydrogen bond increases. The net result is a decrease in $^1J_{N-H}$ from −115.4 Hz when the N−N distance is 3.20 Å, to −101.1 Hz when the N−N distance is 2.40 Å, even though the N−H distance in the proton-donor molecule is constant.

The lower curve in Figure 5 shows the variation of $^1J_{N-H}$ in CNH:NCH as the proton-donor N−H distance is varied while the N−N distance is fixed at 3.30 Å. In Figure 5, $\delta R = 0.00$ Å

corresponds to an N−H distance of 0.90 Å, and this distance increases to 1.70 Å as δR increases to 0.80 Å. As the N−H distance increases, $^1J_{N-H}$ decreases from −116.5 Hz to −72.7 Hz. Once again, the proton-shared character of the hydrogen bond increases as the N−H distance increases and the electron density on the hydrogen-bonded proton decreases. Thus, these data provide some insight into the scatter observed in Figure 2 when $^1K_{X-H}$ is plotted against the X−H distance.

Can the reduced coupling constants $^1K_{X-H}$ and the X−H distances be related? To answer this question, we have plotted these data in a variety of ways. One approach involved an attempt to minimize the dependence of $^1K_{X-H}$ on the specific nature of the proton donor by plotting the ratio K_c/K_m versus R_c/R_m, where K_c and K_m are the reduced X−H coupling constants in the complex and corresponding monomer, respectively, and R_c and R_m are the X−H distances in the complex and monomer, respectively. If these plots are constructed separately for complexes with C−H, N−H, O−H, and F−H donors, a linear relationship is found, as described by the following equations.

For C−H donors:

$$K_c/K_m = -2.10\,R_c/R_m + 3.11$$
$$n = 23;\ r^2 = 0.97$$

For N−H donors:

$$K_c/K_m = -2.44\,R_c/R_m + 3.46$$
$$n = 28;\ r^2 = 0.98$$

For O−H donors:

$$K_c/K_m = -2.95\,R_c/R_m + 3.97$$
$$n = 16;\ r^2 = 0.98$$

For F−H donors:

$$K_c/K_m = -3.89\,R_c/R_m + 4.91$$
$$n = 13;\ r^2 = 0.99$$

There are two interesting observations that can be made from these equations.

1. The difference between the intercept and the absolute value of the slope is essentially the same for the four different proton donors (1.02 for N−H, O−H, and F−H donors; 1.01 for C−H donors.) Although these coefficients have been obtained statistically, they should fit the condition that the sum of the slope and intercept must have a value close to 1 (1 × slope + intercept = 1) since for the monomers, $K_c = K_m$ and $R_c = R_m$.

2. As the X atom of the proton-donor species becomes more electronegative, both the intercepts and the slopes increase.

Plots of the slopes and the intercepts of these 4 equations versus the Pauling electronegativity of X are shown in Figure 6. As evident from this figure, both variables can be related to the Pauling electronegativity through similar second-order curves. We have focused on the slopes, and have further reduced the monomer dependence by subtracting from the reduced coupling constants and distances of complexes the coupling constants and distances of the corresponding monomer. The slopes of four curves that relate $[(R_c - R_m)/R_m]$ to $[(K_c - K_m)/K_m]$ for complexes with C−H, N−H, O−H, and F−H donors are plotted in Figure 7 against the square of the Pauling electronegativity. A linear relationship is found, with a correlation coefficient of 0.999. Thus, the very well-known correlation

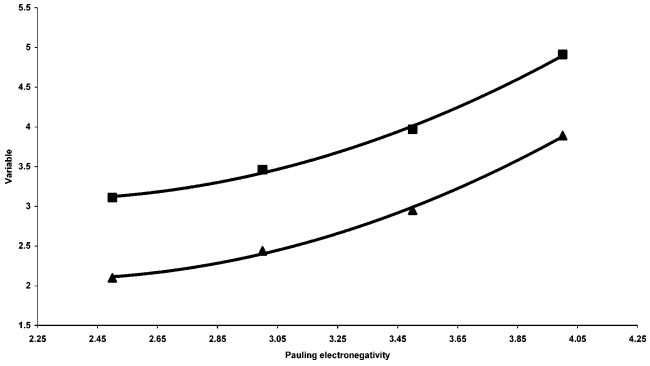

Figure 6. Slopes (◆) and intercepts (■) for straight lines that relate reduced X−H coupling constants to X−H distances plotted against the Pauling electronegativity of X (C, 2.5; N, 3.0; O, 3.5; F, 4.0) For C−H, N−H, O−H, and F−H donors, the plots are of $^1K_{X-H}$ (complex)/$^1K_{X-H}$ (monomer) versus R_{X-H} (complex)/R_{X-H} (monomer).

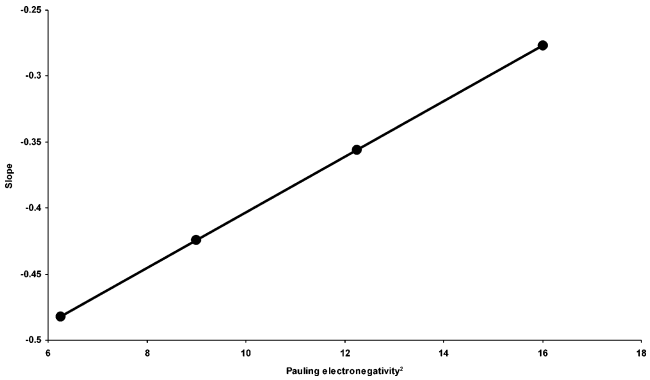

Figure 7. Computed slopes that relate reduced X−H coupling constants to X−H distances plotted against the square of the Pauling electronegativity of X, for complexes with C−H, N−H, O−H, and F−H donors. The slopes relate $[R_{X-H}$ (complex) − R_{X-H} (monomer)]/R_{X-H} (monomer) to $[^1K_{X-H}$ (complex) − $^1K_{X-H}$ (monomer)]/$^1K_{X-H}$ (monomer).

between coupling constants and electronegativity are apparent from these data.[42,45−50]

The relationships evident from Figures 6 and 7 led to the plot shown in Figure 8, which relates the coupling constants for 16 different X−H proton donors and 64 hydrogen-bonded complexes with these donors to the corresponding X−H distances. In Figure 8, $(J_c - J_m)/J_m$ has been plotted against $[(R_c - R_m)/R_m] \times P^2$, where P^2 is the square of the Pauling electronegativity. A linear relationship is found that has a correlation coefficient of 0.97. This relationship is dramatic, given the fact that the same raw data exhibit such scatter in Figure 2, and the recent statement made in ref 42 that it is almost impossible to rationalize trends in measured one-bond spin−spin coupling constants $^1K_{X-H}$ of XH_n hydrides by one simple concept, as has been repeatedly tried in the literature. Moreover, among the many interesting features of this plot is the replacement of the reduced coupling constant ($^1K_{X-H}$) by the coupling constant which would be measured experimentally ($^1J_{X-H}$). This replacement is possible because it is the dimen-

(45) Hruska, F.; Kotowycz, G.; Schefer, T. *Can. J. Chem.* **1965**, *43*, 2827.
(46) Huheey, J. E. *J. Chem. Phys.* **1966**, *45*, 405.
(47) Altona, C.; Ippel, J. H.; Westra Hoekzema, A. J. A.; Erkelens, C.; Groesbeek, M.; Donders, L. A. *Magn. Reson. Chem.* **1989**, *27*, 564.
(48) Berger, S.; Braun, S.; Kalinowski, H.-O. NMR Spectroscopy of the Non-Metallic Elements, John Wiley & Sons: Chichester, 1997, pp 897, 922, 940, 947, 951, 962, 968.
(49) San Fabian, J.; Guilleme, J.; Díez, E. *J. Magn. Reson.* **1998**, *133*, 255.
(50) Clark, T. M.; Grandinetti, P. *J. Solid State NMR* **2000**, *16*, 55.

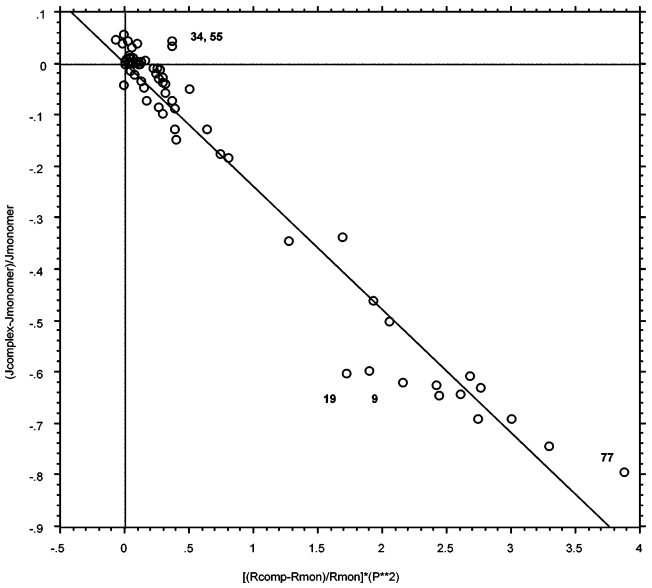

Figure 8. $[^1J_{X-H}\text{ (complex)} - {}^1J_{X-H}\text{ (monomer)}]/{}^1J_{X-H}\text{ (monomer)}$ versus $\{[R_{X-H}\text{ (complex)} - R_{X-H}\text{ (monomer)}]/R_{X-H}\text{ (monomer)}\} \times P^2$, where P^2 is the square of the Pauling electronegativity. Complexes that deviate most from the best-fit straight line are identified according to their number in Table 2.

sionless ratio $(K_c - K_m)/K_m$, which is plotted against $[(R_c - R_m)/R_m] \times P^2$, and the quantity $(K_c - K_m)/K_m$ is equal to $(J_c - J_m)/J_m$. That is, plotting the ratio removes the dependence of the coupling constants on the magnetogyric ratios of X and H. Thus, we have related directly the one-bond coupling constants $^1J_{X-H}$ for complexes with C−H, N−H, O−H, and F−H proton donors. To our knowledge, this is the first time that coupling constants (J) for different pairs of coupled atoms have been related. Figure 8 includes points for the 16 monomers which have the coordinates (0,0) on the graph. To evaluate whether their inclusion skew the data, we replotted the data for the complexes only. Doing this had an imperceptible effect on the appearance of the plot and did not change the correlation coefficient of 0.97.

In Figure 8, the five complexes that deviate most from the best-fit straight line have been indicated by their numbers in Table 2. The five are all charged complexes, including one cation and four anions. The three complexes identified in the lower right of the graph as **19**, **9**, and **77** are $(HNC...H...CNH)^+$, $(NC...H..CN)^-$, and $(F...H...F)^-$, respectively. These complexes have $D_{\infty h}$ symmetry with symmetric proton-shared hydrogen bonds. However, only $(F...H...F)^-$ is an equilibrium structure. The other two have C−H−C hydrogen bonds and are transition structures for proton transfer between two HNC molecules and two CN^- anions, respectively. The constrained structures of these latter two complexes have very long C−H distances. Their deviation from the linear relationship shown in Figure 8 may be due at least in part to these unusually long C−H distances. The two points marked in the upper left of the plot in Figure 8 also correspond to anionic complexes. One is the equilibrium C_1 structure of the complex $NH_3{:}NH_2^-$ (**34**) in which NH_3 is the proton donor to NH_2^-. The second is the equilibrium structure of C_s symmetry for the complex $HOH{:}NC^-$ (**55**). In both of these, the proton-donor N−H and O−H bond lengths are only slightly longer than in the corresponding monomers, which suggests that these two complexes are stabilized by traditional hydrogen bonds. Of the five complexes that deviate most from the linear behavior illustrated in Figure 8, points for three of them lie above the line, while two lie below. As a result, omitting all anions, or all nonequilibrium structures, or both, does not improve the correlation coefficient of 0.97 for the entire set. An analysis of the residuals shows no trend other than the larger residuals found for complexes in the lower-right corner of the plot where the confidence intervals for the slope are greater. These complexes are those with increased proton-shared character of the hydrogen bond.

As noted above, the second striking feature of Figure 2 is the fact that all reduced one-bond X−H coupling constants are positive, both in the monomers and in the hydrogen-bonded complexes. Since the FC term dominates in all cases, it is justified to analyze $^1K_{X-H}$ by analyzing the reduced Fermi-contact terms, which are also large and positive for all X−H bonds. The nuclear magnetic resonance triplet wave function model (NMRTWM)[9] states that the sign of $^1K_{X-H}$ (more precisely the sign of the reduced FC term) is a result of competing positive and negative contributions from excited triplet σ-type states of the appropriate symmetry that couple to the ground state through the Fermi-contact operator. The orientations of the nuclear magnetic moments of the coupled atoms repond to the phases of the triplet-state wave functions, such that if the phases at two atoms are the same (both positive or both negative), then the alignment of the nuclear moments is parallel, and the sign of the reduced FC term is negative. In contrast, if the signs of the wave function at two nuclei are different, then their nuclear magnetic moments have an antiparallel alignment, and the sign of the FC term is positive. Since all FC terms (and therefore $^1K_{X-H}$) for X−H coupling are positive, this implies that states with one node (or an odd number of nodes) intersecting the X−H bond dominate.

Because all reduced one-bond X−H coupling constants ($^1K_{X-H}$) in the proton-donor molecules are positive, it is possible to predict the signs of $^1J_{X-H}$ by noting the signs of the magnetogyric ratios of X and H. Since ^{1}H has a positive magnetogyric ratio, the sign of $^1J_{X-H}$ depends on the sign of the magnetogyric ratio of X. This means that $^1J_{C-H}$ and $^1J_{F-H}$ will be positive, while $^1J_{N-H}$ and $^1J_{O-H}$ will be negative. This generalization is evident from Figure 1, which shows that points for $^1J_{N-H}$ and $^1J_{O-H}$ are found in the lower left quadrant of the plot, while those for $^1J_{C-H}$ and $^1J_{F-H}$ are in the upper right.

In our previous paper, we noted that reduced-two bond X−Y spin−spin coupling constants across X−H−Y hydrogen bonds ($^{2h}K_{X-Y}$) are also positive,[1] with the exception of $^{2h}K_{F-F}$ in $(HF)_2$. With respect to the lower-energy triplet states, this means that the dominant states have one node intersecting either the X−H covalent bond or the H...Y hydrogen bond. Which of these two is the more important cannot be determined without a complete sum-over-states calculation, which is not feasible.[44] Although it is not necessary that the same states that determine the sign of $^1K_{X-H}$ should also be responsible for determining the sign of $^{2h}K_{X-Y}$ in a particular hydrogen-bonded complex, this is certainly a possibility. The dominant low-energy states for both could be those that have one node (or an odd number of nodes) intersecting the X−H covalent bond and no nodes (or an even number of nodes) intersecting the H−Y hydrogen bond.

Conclusions

A systematic study of one-bond spin−spin coupling constants for a series of monomers and hydrogen-bonded complexes has been carried out using the ab initio EOM-CCSD method. The results of this study of $^{13}C-^1H$, $^{15}N-^1H$, $^{17}O-^1H$, and $^{19}F-^1H$ coupling constants for a set of 16 monomers and 64 hydrogen-bonded complexes in which these monomers are proton donors support the following statements.

1. There is good agreement between the computed monomer coupling constants and available experimental data.

2. All reduced one-bond spin−spin coupling constants ($^1K_{X-H}$) for the monomers and complexes are positive. Since the magnetogyric ratio of ^1H is positive, this implies that $^1J_{C-H}$ and $^1J_{F-H}$ are positive, while $^1J_{N-H}$ and $^1J_{O-H}$ are negative, in agreement with experimental data. Insight into the positive signs of the reduced coupling constants can be obtained through the NMR Triplet Wave function Model (NMRTWM).

3. It is not possible to relate $^1K_{X-H}$ to X−H distances directly, since a plot of these quantities exhibits significant scatter. However, by reducing the dependence on the specific monomer and relating $^1K_{X-H}$ to the Pauling electronegativity, a plot of the ratio of coupling constants for complexes and monomers versus the ratio of X−H distances for complexes and monomers times the square of the Pauling electronegativity produces a straight line with a correlation coefficient of 0.97. Since the ratio removes the dependence of coupling constants on the magnetogyric ratios of X and H, $^1K_{X-H}$ and $^1J_{X-H}$ produce the same straight line. For the first time, coupling constants for four different pairs of atoms (C−H, N−H, O−H, and F−H) have been simply related to X−H distances and the Pauling electronegativity of X.

4. The five complexes that exhibit the largest deviations from the linear relationship described in point 3 are charged complexes, 4 anions, and 1 cation. Three have symmetric proton-shared hydrogen bonds. Of these, the two that exhibit the greatest deviation from linearity are constrained transition structures for proton transfer that have unusually long C−H distances.

5. Detailed analyses of the variation of N−H coupling constants and proton chemical shifts in selected monomers and complexes indicate that it is not simply the X−H distance that influences X−H spin−spin coupling constants in complexes. Rather, as the X−H distance increases, the proton-shared character of the hydrogen bond also increases, and the electron density on the hydrogen-bonded proton decreases. This leads to a decrease in the reduced X−H coupling constant.

Acknowledgment. This work was supported by a grant from the U.S. National Science Foundation (NSF CHE-9873815) and by the Spanish DGI/MCyT (project no. BQU-2003-01251). The authors gratefully acknowledgment this support, and that of the Ohio Supercomputer Center.

JA0401545